Differential expression of sphingolipids in P-glycoprotein or multidrug resistance-related protein 1 expressing human neuroblastoma cell lines

Anne-Jan Dijkhuis[a,b], Jenny Douwes[c], Willem Kamps[b], Hannie Sietsma[c], Jan Willem Kok[a,*]

[a] *Department of Membrane Cell Biology, Groningen University Institute for Drug Exploration (GUIDE), University of Groningen, A. Deusinglaan 1, Bldg. 3215, 10th Fl., 9713 AV Groningen, The Netherlands*
[b] *Division of Pediatric Oncology, Department of Pediatrics, Beatrix Children's Hospital, Hanzeplein 1, 9713 GZ Groningen, The Netherlands*
[c] *Department of Pathology, University Hospital Groningen, Hanzeplein 1, 9713 GZ Groningen, The Netherlands*

Received 5 May 2003; revised 16 June 2003; accepted 18 June 2003

First published online 1 July 2003

Edited by Guido Tettamanti

Abstract The sphingolipid composition and multidrug resistance status of three human neuroblastoma cell lines were established. SK-N-FI cells displayed high expression and functional (efflux) activity of P-glycoprotein, while multidrug resistance-related protein 1 was relatively abundant and most active in SK-N-AS cells. These two cell lines exhibited higher sphingolipid levels, compared to SK-N-DZ, which had the lowest activity of either ATP-binding cassette transporter protein. SK-N-DZ cells also differed in ganglioside composition with predominant expression of b-series gangliosides. In conclusion, these three neuroblastoma cell lines offer a good model system to study sphingolipid metabolism in relation to ATP-binding cassette transporter protein function.

Key words: Neuroblastoma; Sphingolipid; Ganglioside; Multidrug resistance; P-glycoprotein; Multidrug resistance-related protein 1

1. Introduction

Treatment failure in neuroblastoma, one of the most common extracranial solid tumors in childhood, is often due to the occurrence of multidrug resistance (MDR). A large variety of MDR mechanisms exists, including the overexpression of energy-dependent drug efflux proteins, such as P-glycoprotein (Pgp) and multidrug resistance-related protein 1 (MRP1) [1].

Moreover, it has become apparent that sphingolipids and their metabolism play a role in drug resistance, possibly in concert with ATP-binding cassette (ABC) transporter proteins [2–4]. Evidence for a relation between MDR and sphingolipids has come from studies in tumor cell lines, which acquired a drug resistant phenotype by selection with cytotoxic agents. The level of glucosylceramide (GlcCer), a precursor of all complex glycosphingolipids and a direct metabolic product of ceramide (Cer), was consistently elevated in several Pgp overexpressing cell lines [5]. A similar GlcCer increase was observed in the MRP1 overexpressing HT29^{col} cell line [6]. It has even been suggested to consider increased GlcCer levels as a diagnostic marker for MDR tumors [7].

Little is known concerning the mechanisms underlying MDR-associated sphingolipid changes, but these may depend on cell type. It has been suggested that increased conversion of Cer to GlcCer by glucosylceramide synthase (GCS) in Pgp overexpressing MCF-7 cells rescues cells from cytostatic-induced Cer-mediated apoptosis [8,9]. On the other hand, in Pgp overexpressing 2780AD cells, uncoupling of GlcCer and lactosylceramide (LacCer) biosynthesis in the Golgi apparatus leads to accumulation of GlcCer, without changes in GCS expression or activity [10]. It is therefore important to explore MDR-associated changes in sphingolipid composition in a wide variety of tumor cells with variable expression of ABC transporter proteins.

In this study we have characterized both the MDR status and the sphingolipid composition of three human neuroblastoma cell lines, SK-N-AS, SK-N-DZ and SK-N-FI. These cell lines offer the advantage that their MDR properties have emerged in vivo, in contrast to in vitro drug selection models. In the latter multiple cellular adaptations may have been co-selected. An additional advantage of these cell lines is their high content of complex glycosphingolipids, e.g. gangliosides [11]. Although gangliosides have only rarely been associated with MDR, a recent study in human myeloblastic KG1a/200 cells shows GM3- and GD3-induced phosphorylation of Pgp on serine residues, thereby modulating its activity [12].

Our results in these neuroblastoma cell lines show that differential neutral sphingolipid and ganglioside metabolism occur in a background of differential Pgp and MRP1 expression and activity, acquired in vivo. As such, this contributes to our knowledge of MDR-associated sphingolipid metabolism. In addition, this offers a good model to study the contribution of specific sphingolipids, including specific gangliosides, to drug resistance of tumor cells.

2. Materials and methods

2.1. Cell culture conditions

Human neuroblastoma cell lines SK-N-AS, SK-N-DZ and SK-N-FI were purchased from the ATCC (Manassas, VA, USA). They were

*Corresponding author. Fax: (31)-50-3632728.
E-mail addresses: a.dijkhuis@med.rug.nl (A.-J. Dijkhuis), w.a.kamps@bkk.azg.nl (W. Kamps), j.sietsma@path.azg.nl (H. Sietsma), j.w.kok@med.rug.nl (J.W. Kok).

Abbreviations: ABC, ATP-binding cassette; BF, efflux-blocking factor; Cer, ceramide; CFDA, 5-carboxyfluorescein diacetate; CSA, cyclosporin A; GalCer, galactosylceramide; GCS, glucosylceramide synthase; GlcCer, glucosylceramide; HPTLC, high-performance thin layer chromatography; LacCer, lactosylceramide; MDR, multidrug resistance; MRP1, multidrug resistance-related protein 1; Pgp, P-glycoprotein; Rh123, Rhodamine 123; SM, sphingomyelin

0014-5793/03/$22.00 © 2003 Published by Elsevier Science B.V. on behalf of the Federation of European Biochemical Societies.
doi:10.1016/S0014-5793(03)00721-X

Table 1
Efflux-blocking factors (BF) for Pgp and MRP1 in human neuroblastoma cell lines

	BF			*P*-values	
	Pgp	MRP1		Pgp	MRP1
SK-N-AS	2.2 ± 0.4	26.7 ± 18.2	AS v DZ	0.02	0.03
SK-N-DZ	1.7 ± 0.3	5.3 ± 2.9	AS v FI	< 0.001	0.01
SK-N-FI	86.0 ± 23.9	8.5 ± 2.6	DZ v FI	< 0.001	0.07

Cells were loaded with either Rh123 (10 μM) or CFDA (0.5 μM) for 60 min at 37°C or 10°C, followed by efflux in the presence or absence of the inhibitors CSA (10 μM) or MK571 (20 μM) for 60 min or 45 min at 37°C. BF were calculated as described in Section 2. Data represent the mean ± S.D. of four independent experiments.

grown as adherent monolayer cultures in Dulbecco's modified Eagle's medium (Gibco, Life Technologies BV, Breda, The Netherlands) supplemented with 10% fetal calf serum (Bodinco, Alkmaar, The Netherlands), 100 units/ml penicillin (Gibco), 100 μg/ml streptomycin (Gibco) and non-essential amino acids (Gibco), under standard incubator conditions (humidified atmosphere, 95% air, 5% CO_2, 37°C).

2.2. Detection of Pgp and MRP1 expression by Western blot analysis

Western blot analysis was performed as described [6]. Briefly, cells were washed and subjected to protein content determination (Biorad, Veenendaal, The Netherlands). Ten μg of protein dissolved in sample buffer was heated for 5 min at 95°C (except MRP1 samples), loaded and run on SDS–PAGE (sodium dodecyl sulfate–polyacrylamide gel electrophoresis; 10%) mini-gels. Proteins were electrotransferred onto Immobilon-P PVDF. For detection, primary mouse anti-Pgp, C219 (Signet-Sanbio B.V., Uden, The Netherlands), 1:300 or rat anti-MRP1, MRPr1 (Signet-Sanbio B.V.), 1:1000 antibodies and secondary alkaline phophatase-conjugated sheep anti-mouse (Pgp) or anti-rat (MRP1) IgG antibodies (Boehringer Mannheim GmbH, Mannheim, Germany) were used. Immunoreactive proteins were detected using *p*-nitroblue tetrazolium and 5-bromo-4-chloro-3-indolyl phosphate as substrates.

2.3. Measurement of cellular sensitivity to cytotoxic drugs (MTT assay)

Fifteen thousand cells/well were plated in microtiter plates. Cytostatics were added 4 h after plating. Ninety-six hours after plating viability of the cells was determined as previously described [13]. Briefly, 100 μg of MTT (Sigma, St. Louis, MO, USA) was added to each well and cells were incubated for 3.5 h at 37°C. Plates were then centrifuged (15 min, 900×*g*) and the supernatants were removed. Pellets were dissolved in DMSO and absorbencies were measured in a microtiter plate reader (μQuant, Bio-Tek Instruments, Winooski, VT, USA) at a λ of 570 nm. The background absorbency was subtracted from all values and data were expressed as percentage compared to untreated control cells (= 100%). IC_{50} values (= drug concentration which results in viability reduction of 50%) were determined directly from the dose–response curves.

2.4. Detection of Pgp and MRP1-mediated drug efflux by FACS analysis

Cells (1×10^6 in HBSS) were incubated for 60 min at 37°C in the presence of the Pgp substrate Rhodamine 123 (Rh123, 10 μM, Sigma) or the MRP1 substrate 5-carboxyfluorescein diacetate (CFDA, 0.5 μM, Sigma) and in the presence '(+/+)' or absence '(−/−)' of the Pgp inhibitor cyclosporin A (CSA, 10 μM, Alexis, Carlsbad, CA, USA) or the MRP1 inhibitor MK571 (20 μM). After loading, cells were washed with ice-cold buffer and incubated for 60 min (Pgp) or 45 min (MRP1) at 37°C (efflux) in the presence (+/+) or absence (−/−) of inhibitor. Subsequently, efflux was stopped by replacement with ice-cold buffer and Rh123/CF fluorescence was measured by flow cytometry (FACSCalibur; Becton Dickinson, Franklin Lakes, NJ, USA). For each sample 5000 events were collected and analyzed using Win-list 5.0 software (Verity Software House Inc., Topsham, ME, USA), which resulted in median relative fluorescence units (F.U.). From these data the efflux-blocking factor (BF) was calculated, which is defined as:

$$\mathrm{BF} = \frac{[\text{F.U. in } (+/+)\text{cells} - \text{F.U. in untreated cells}]}{[\text{F.U. in } (-/-)\text{cells} - \text{F.U. in untreated cells}]}$$

2.5. Equilibrium radiolabeling and analysis of cellular sphingolipids

Sphingolipid pools were metabolically radiolabeled to equilibrium as described [10]. Cells were grown for 48 h in the presence of L-[U-^{14}C]serine (1 μCi/ml; Amersham International, Bercks, UK), harvested and subjected to lipid extraction [14]. Acylglycerolipids were hydrolyzed during 1 h incubation at 37°C in $CHCl_3/CH_3OH$ (1:1, v/v) containing NaOH (0.1 M). The remaining lipids were re-extracted and applied on high-performance thin layer chromatography (HPTLC) plates (Merck, Amsterdam, The Netherlands). Plates were developed in $CHCl_3/CH_3OH/H_2O$ (14:6:1, v/v/v) in the first dimension and in $CHCl_3/CH_3COOH$ (9:1, v/v) in the second dimension. After scraping of the Cer containing spots, the plates were sprayed with 2.5% H_3BO_3 (w/v) in CH_3OH and developed once more in the second dimension, this time using $CHCl_3/CH_3OH$/25% (w/v) NH_4OH (13:7:1, v/v/v) as the mobile phase. GlcCer, galactosylceramide (GalCer), LacCer, and sphingomyelin (SM) containing spots were scraped from the plates. Radioactivity was measured by scintillation counting (Packard Topcount microplate scintillation counter, Meriden, CT, USA). Lipid levels were expressed as dps incorporated in a specific lipid species per 10^3 dps of total lipid-incorporated radioactivity, as measured after the initial lipid extraction.

2.6. Measurement of C_5-Bodipy-labeled sphingolipids

Cells were washed three times with HBSS and incubated in the presence of C_5-Bodipy-ceramide (4 μM; Molecular Probes Europe BV, Leiden, The Netherlands) at 37°C for 3 h. After washing, cells were scraped, the protein content was determined and lipids were extracted [14]. Extracted lipids were applied to HPTLC plates and run in $CHCl_3/CH_3OH/NH_4OH/H_2O$ (60:40:4:1; v/v/v/v). Individual spots were scraped, suspended in a 1% (v/v) Triton X-100 solution (2 ml), and shaken vigorously for 1 h. After centrifugation, fluorescence in the supernatants was measured (λ_{ex} = 505 nm; λ_{em} = 511 nm; SLM Aminco SPF-500, Urbana, IL, USA), by reference to a standard curve of a known amount of C_5-Bodipy-Cer.

2.7. Mass analysis of gangliosides

Gangliosides were isolated from $5–7\times10^7$ cells, as described [15,16]. Briefly, pelleted cells were extracted in $CHCl_3/CH_3OH$ (1:1; v/v) and $CHCl_3/CH_3OH$ (2:1; v/v). Pooled supernatants were dried (N_2) and the lipids were dissolved and sonicated in $CHCl_3/CH_3OH$ (1:1; v/v). After centrifugation and overnight storage at −20°C, the supernatant was dried, dissolved in diisopropylether/1-butanol (3:2; v/v), and 17 mM NaCl was added. The aqueous phase was re-extracted with diisopropylether/1-butanol and subsequently lyophilized. Samples were dissolved in CH_3OH/H_2O (1:1; v/v) and loaded onto pre-washed Sep-

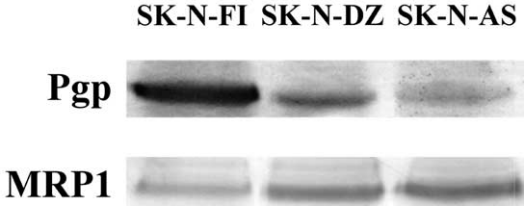

Fig. 1. Western blot of relative Pgp or MRP1 expression levels in human neuroblastoma cell lines. Equal amounts of protein were loaded on the gel. The sizes of the Pgp and MRP1 proteins are 170 and 190 kDa, respectively. Shown are representative results from at least three independent experiments.

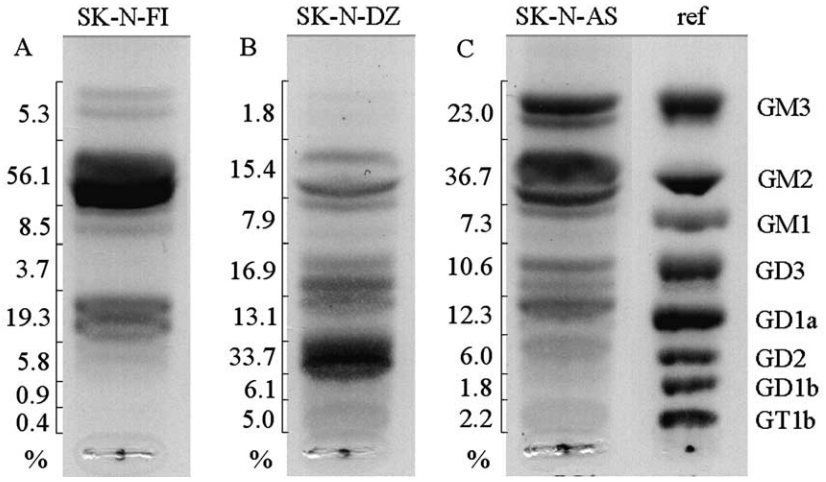

Fig. 2. A–C: Ganglioside patterns of the human neuroblastoma cell lines SK-N-FI, SK-N-DZ and SK-N-AS, respectively. Reference gangliosides (ref) and the relative amount of gangliosides per cell line are displayed next to these patterns. Ganglioside quantification was done by densitometry. The cell lines SK-N-FI (89%) and SK-N-AS (79%) predominantly express a-series gangliosides (GM3, GM2, GM1 and GD1a), while b-series gangliosides (GD3, GD2, GD1a and GT1b) are the major products (62%) of the SK-N-DZ cell line. Gangliosides were isolated from aliquots of cells with equal protein content. Shown are representative results from three independent experiments.

Pak C_{18} (Waters, Milford, MA, USA) cartridges. After rinsing (H_2O), gangliosides were eluted with CH_3OH and $CHCl_3/CH_3OH$ (1:1; v/v). The eluate was concentrated and loaded onto HPTLC plates, which were developed in $CHCl_3/CH_3OH$/0.2% (w/v) $CaCl_2$ (11:9:2; v/v/v) and stained with Ehrlich reagent [17]. Gangliosides were quantified by densitometry, involving analysis with Scion Image Beta 4.0.2 (Scion Corporation, Frederick, MD, USA) software of a scanned image of the HPTLC.

2.8. Statistical analysis

Results are presented as mean ± S.D. ($n \geq 4$). Statistical analysis was performed with the Student's *t*-test, considering $P < 0.05$ significant.

3. Results

3.1. Differential Pgp and MRP1 expression and efflux activity in SK-N-FI, SK-N-DZ and SK-N-AS

Western blotting analysis revealed the relative expression levels of Pgp and MRP1 in three human neuroblastoma cell lines (Fig. 1). Pgp expression was high in SK-N-FI, and low in SK-N-AS. In contrast, MRP1 expression was highest in SK-N-AS and lowest in SK-N-FI. SK-N-DZ displayed intermediate levels of both ABC transporters. In accordance, significant (Rh123) efflux activity of Pgp was observed in SK-N-FI cells only (Table 1). Moreover, significant functional activity of MRP1 was found in SK-N-AS, while SK-N-FI and SK-N-DZ displayed residual efflux activity.

3.2. Functional activity of ABC transporters is correlated with resistance to multiple cytotoxic drugs

The impact of functional (efflux) activity of ABC transporters on drug resistance was explored by means of cytotoxicity assays. The three cell lines were exposed to taxol, vincristine, etoposide and doxorubicin, which have all been recognized as Pgp substrates. Accordingly, the Pgp expressing SK-N-FI displayed relatively high resistance to all four cytostatic drugs, with high IC_{50} values (Table 2). The MRP1 expressing SK-N-AS was less resistant even though MRP1 is able to transport vincristine, etoposide and doxorubicin. Least resistance was displayed by SK-N-DZ, which lacked significant functional activity of either Pgp or MRP1.

In conclusion, the highest expression levels and activities of Pgp and MRP1 were found in the SK-N-FI and SK-N-AS cell lines, respectively. This expression correlated well with the degree of drug resistance displayed by these neuroblastoma cell lines, compared to SK-N-DZ, and suggests a prominent role for ABC transporters, especially Pgp, in drug resistance of these cell lines.

3.3. Analysis of the sphingolipid composition in SK-N-AS, SK-N-DZ and SK-N-FI cells

Sphingolipid biosynthesis was studied by incubating the cells with C_5-Bodipy-Cer. A relatively high conversion to both C_5-Bodipy-GlcCer and C_5-Bodipy-SM was observed in both SK-N-FI and SK-N-AS, as compared to SK-N-DZ (Table 3A). The high conversion to C_5-Bodipy-SM correlated well with high endogenous levels of SM in SK-N-FI and especially SK-N-AS, as measured by equilibrium radiolabeling (Table 3B). Endogenous GlcCer, which is known to be associated with MDR, is more abundant as well in the resistant

Table 2
IC_{50} values for taxol, vincristine, etoposide and doxorubicin as determined with the MTT cell survival assay

	Taxol (nM)	Vincristine (ng/ml)	Etoposide (ng/ml)	Doxorubicin (nM)
SK-N-AS	6.8 ± 3.5	0.8 ± 0.3	875 ± 114	291 ± 72
SK-N-DZ	2.0 ± 0.1	0.9 ± 0.2	213 ± 6	85 ± 5
SK-N-FI	> 50	> 30	> 1000	> 1000

SK-N-AS, SK-N-DZ and SK-N-FI were exposed to increasing concentrations of taxol (0–50 nM), vincristine (0–30 ng/ml), etoposide (0–1000 ng/ml) and doxorubicin (0–1000 nM) for 96 h. Data represent the mean ± S.D. of four or more than four independent experiments, each consisting of two replicate determinations.

Table 3
Sphingolipid metabolism and composition of SK-N-FI, SK-N-DZ and SK-N-AS, as determined with the use of C_5-Bodipy-Cer and L-[U-^{14}C]serine, respectively

	SK-N-FI	SK-N-DZ	SK-N-AS
(A) C_5-Bodipy-labeled lipids			
GlcCer	29.9 ± 5.9	17.1 ± 1.3	27.0 ± 7.4
SM	27.3 ± 2.7	19.5 ± 5.7	65.8 ± 15.1
(B) Radiolabeled lipids			
Cer	12.9 ± 2.3	9.8 ± 1.0	7.4 ± 1.0
GlcCer	10.1 ± 1.1	4.2 ± 1.3	8.2 ± 0.9
LacCer	11.6 ± 1.9	4.0 ± 0.6	1.8 ± 0.2
GalCer	1.7 ± 0.4	0.8 ± 0.4	1.4 ± 0.1
SM	45.0 ± 1.2	16.6 ± 5.1	74.1 ± 7.2

(A) Cells were incubated with C_5-Bodipy-Cer (4 μM) for 3 h and lipids were isolated and analyzed. The amounts of newly synthesized C_5-Bodipy-GlcCer and C_5-Bodipy-SM were calculated in nmol lipid/mg protein from six independent experiments. (B) Cells were incubated with L-[U-^{14}C]serine (1 μCi/ml) for 48 h and sphingolipids were isolated and analyzed. Values are expressed as dps of a specific sphingolipid per 1000 dps of the total radiolabeled lipid pool. Data represent the mean ± S.D. of four independent experiments.

SK-N-FI and SK-N-AS, as compared to the relatively chemosensitive SK-N-DZ.

The three cell lines were also analyzed for their ganglioside composition (Fig. 2). High levels of a-series (i.e. GM3, GM2, GM1 and GD1a) gangliosides were found in SK-N-FI (Fig. 2A) and SK-N-AS (Fig. 2C). In contrast, the SK-N-DZ (Fig. 2B) expressed predominantly b-series gangliosides (GD3, GD2, GD1b and GT1b).

4. Discussion

It has been shown that in vitro established Pgp [5,10] and MRP1 [6] overexpressing tumor cell lines display enhanced levels of the sphingolipid GlcCer. Moreover, these studies showed that in addition to changes in the level of GlcCer, other sphingolipid levels are altered in MDR tumor cells, however in a cell-type-dependent fashion. In the present study, we analyzed the composition and metabolism of sphingolipids in neuroblastoma cell lines, which differ from the previously studied models in the sense that MDR acquisition and ABC transporter expression were attained in vivo, and thus more resemble naturally occurring adaptations. In this model, an enhanced GlcCer level also parallels expression of functionally active ABC transporters, and additional changes in sphingolipid composition occur as well. A novel finding in the current model is that expression of ABC transporters is correlated with overall enhanced levels and biosynthesis of sphingolipids, while a dichotomy is observed with respect to the biosynthetic pathway of choice. Although Pgp is expressed in all three neuroblastoma cell lines, it is functionally active only in SK-N-FI and this is correlated with channelling of sphingolipid metabolism into glycolipids. MRP1 is also expressed in all three cell lines, but functional activity only occurs in SK-N-AS. The latter is correlated with channeling of sphingolipid metabolism towards SM biosynthesis. A direct causal relationship between sphingolipid metabolism and ABC transporter expression/function remains to be proven. With respect to the downstream metabolic products of GlcCer, such as gangliosides, differences were also observed between functionally active ABC transporter expressing neuroblastoma cells and SK-N-DZ cells. The high expression of GD2, as occurs in SK-N-DZ, is generally associated with more aggressive forms of neuroblastoma, but relations to drug resistance are unknown. A functional role for gangliosides in MDR is only recently emerging. Certain gangliosides (GM3, GD3) may be directly involved in MDR by modulation of Pgp function through alteration of its phosphorylation state [12]. Consistent with this notion, our preliminary results in the SK-N-AS cell line show that long-term (5 days) inhibition of glycolipid synthesis by incubation with 1-phenyl-2-hexadecanoylamino-3-pyrrolidino-1-propanol results in a 30% decrease of MRP1-mediated CF efflux (data not shown). Recently, up-regulation of ganglioside biosynthesis at the level of GM3 biosynthesis was shown to occur in fenretinide-adapted A2780 cells, and was correlated with fenretinide resistance [18]. Due to the novelty of this particular research area and the limited studies and results available, a consistent picture concerning the contribution of specific gangliosides to MDR has not yet emerged.

In conclusion, the three neuroblastoma cell lines characterized in this study offer a good model to further dissect the roles of specific sphingolipids and their metabolism in MDR at various levels of sphingolipid metabolic pathways and against a background of either one of the two most established MDR-associated functional ABC transporters.

Acknowledgements: This work was supported by a grant from the Groningen Foundation of Pediatric Oncology (KOCG 99-03). We thank Merck Frosst Canada Inc. (Quebec, Canada) for the generous gift of MK571.

References

[1] McKenna, S.L. and Padua, R.A. (1997) Br. J. Haematol. 96, 659–674.
[2] Sietsma, H., Veldman, R.J. and Kok, J.W. (2001) J. Membr. Biol. 181, 153–162.
[3] Senchenkov, A., Litvak, D.A. and Cabot, M.C. (2001) J. Natl. Cancer Inst. 93, 347–357.
[4] Sietsma, H., Dijkhuis, A.J., Kamps, W.A. and Kok, J.W. (2002) Neurochem. Res. 27, 665–674.
[5] Lavie, Y., Cao, H., Bursten, S.L., Giuliano, A.E. and Cabot, M.C. (1996) J. Biol. Chem. 271, 19530–19536.
[6] Kok, J.W., Veldman, R.J., Klappe, K., Koning, H., Filipeanu, C.M. and Muller, M. (2000) Int. J. Cancer 87, 172–178.
[7] Lucci, A., Cho, W.I., Han, T.Y., Giuliano, A.E., Morton, D.L. and Cabot, M.C. (1998) Anticancer Res. 18, 475–480.
[8] Liu, Y.Y., Han, T.Y., Giuliano, A.E. and Cabot, M.C. (1999) J. Biol. Chem. 274, 1140–1146.
[9] Liu, Y.Y., Han, T.Y., Giuliano, A.E. and Cabot, M.C. (2001) FASEB J. 15, 719–730.
[10] Veldman, R.J., Klappe, K., Hinrichs, J., Hummel, I., van der Schaaf, G., Sietsma, H. and Kok, J.W. (2002) FASEB J. 16, 1111–1113.

[11] Kaucic, K., Etue, N., LaFleur, B., Woods, W. and Ladisch, S. (2001) Cancer 91, 785–793.
[12] Plo, I., Lehne, G., Beckstrom, K.J., Maestre, N., Bettaieb, A., Laurent, G. and Lautier, D. (2002) Mol. Pharmacol. 62, 304–312.
[13] Carmichael, J., Degraff, W.G., Gazdar, A.F., Minna, J.D. and Mitchel, J.B. (1987) Cancer Res. 47, 936–942.
[14] Bligh, E.J. and Dyer, W.J. (1959) Can. J. Biochem. Physiol. 13, 911–917.
[15] Senn, H.J., Orth, M., Fitzke, E., Wieland, H. and Gerok, W. (1989) Eur. J. Biochem. 181, 657–662.
[16] Ladisch, S. and Gillard, B. (1985) Anal. Biochem. 146, 220–231.
[17] Partridge, S.M. (1948) Biochem. J. 42, 238–248.
[18] Prinetti, A., Basso, L., Appierto, V., Villani, M.G., Valsecchi, M., Loberto, N., Prioni, S., Chigorno, V., Cavadini, E., Formelli, F. and Sonnino, S. (2003) J. Biol. Chem. 278, 5574–5583.